Histological Evidence of Muscle Degeneration in Advanced Human Rotator Cuff Disease

Michael C. Gibbons, MS, Anshu Singh, MD, Oke Anakwenze, MD, Timothy Cheng, MD, Maxwill Pomerantz, BS, Simon Schenk, PhD, Adam J. Engler, PhD, and Samuel R. Ward, PT, PhD

Investigation performed at the University of California, San Diego, San Diego, California

Background: Cellular remodeling in rotator cuff muscles following a massive rotator cuff tear is poorly understood. The aim of the current study was to provide histological evidence to elucidate the mode of muscle loss in advanced human rotator cuff disease and to assess tissue-level changes in relation to findings on noninvasive imaging.

Methods: Rotator cuff muscle biopsy samples were taken from the scapular fossae from 23 consecutive patients undergoing reverse total shoulder arthroplasty in order to evaluate muscle composition in severe rotator cuff disease. Markers of vascularity; inflammation; fat distribution; and muscle atrophy, degeneration, and regeneration were quantified.

Results: The samples primarily consisted of dense, organized connective tissue (48.2% ± 19.1%) and disorganized, loose connective tissue (36.9% ± 15.9%), with substantially smaller fractions of muscle (10.4% ± 22.0%) and fat (6.5% ± 11.6%). Only 25.8% of the biopsy pool contained any muscle fibers at all. Increased inflammatory cell counts (111.3 ± 81.5 macrophages/mm^2) and increased vascularization (66.6 ± 38.0 vessels/mm^2) were observed across biopsies. Muscle fiber degeneration was observed in 90.0% ± 15.6% of observable muscle fascicles, and the percentage of centrally nucleated muscle fibers was pathologically elevated (11.3% ± 6.3%). Fat accumulation was noted in both perifascicular (60.7% ± 41.4%) and intrafascicular (42.2% ± 33.6%) spaces, with evidence that lipid may replace contractile elements without altering muscle organization.

Conclusions: Dramatic degeneration and inflammation of the rotator cuff muscles are characteristics of the most chronic and severe rotator cuff disease states, suggesting that muscle loss is more complicated than, and distinct from, the simple atrophy found in less severe cases.

Clinical Relevance: In order to address degenerative muscle loss, alternative therapeutic approaches directed at muscle regeneration must be considered if muscle function is to be restored in late-stage rotator cuff disease.

Peer review: This article was reviewed by the Editor-in-Chief and one Deputy Editor, and it underwent blinded review by two or more outside experts. The Deputy Editor reviewed each revision of the article, and it underwent a final review by the Editor-in-Chief prior to publication. Final corrections and clarifications occurred during one or more exchanges between the author(s) and copyeditors.

The lifetime prevalence of rotator cuff tear is estimated to be as high as 20% of the general population, where risk increases significantly with age[1]. Because rotator cuff tears may remain asymptomatic for years, and the onset of symptoms is often insidious, many patients do not seek treatment until the disease has progressed to a more chronic state. When accompanied by other factors such as smoking, diabetes, and age, this late-stage intervention results in surgical failure rates as high as 50%[2]. While the composition, quality, and function of the muscle in rotator cuff disease plays an important role in disease progression and recovery potential, the biological features of the muscle remain poorly defined on the cellular level, particularly in late-stage disease.

Relative to muscle, the response of the rotator cuff tendons to tear has been better studied biomechanically, biochemically, and histologically[3-5]. Those studies suggested that, while the tendon may look healthy macroscopically, at the cellular and molecular level, the torn tendon is degenerated, with signs including increased vascularity, adipose content, inflammation, and apoptosis[3-5]. We hypothesized that, as rotator cuff disease progresses, muscle as well as tendon is lost to degenerative processes. Specifically, in advanced rotator cuff disease, we

Disclosure: Financial support for this work was provided by the National Institutes of Health (NIH) R01 HD073180 (S.R.W.); the Orthopaedic Research and Education Foundation (OREF) Resident Research Grant (T.C.); and the University of California, San Diego Frontiers of Innovation Scholars Program Fellowship (M.C.G.). The **Disclosure of Potential Conflicts of Interest** forms are provided with the online version of the article.

TABLE I Patient Demographics*

	Patient Age† (yr)	Sex (no.)		Massive Tear (no. [%])	Average Goutallier Score (No. of Samples)			
		M	F		Supraspinatus	Infraspinatus	Teres Minor‡	All
Total cohort	73.9 ± 8.3	10	13	19/23 (83%)	2.9 (18)	2.7 (11)	1.5 (2)	2.7 (31)
Muscle-containing samples	75.8 ± 10.7	3	5	7/8 (88%)	3.0 (2)	2.8 (4)	1.5 (2)	2.5 (8)

*N = 23 patients. A total of 31 samples were obtained for biopsy; 8 (26%) contained histologically identifiable muscle fibers. †The values are given as the mean and the standard deviation. ‡Biopsy samples taken from the intersection of the infraspinatus and teres minor in a position where the muscles are difficult to differentiate.

expected to see a degenerative muscle phenotype demonstrating disrupted muscle fiber structure, myophagocytosis, and increased central nuclei, all signs of muscle degeneration-regeneration[6] not reported in earlier disease states.

While *atrophy* and *degeneration* are distinct mechanisms of muscle loss often involving different pathways and drivers[7-9], the terms *fatty atrophy, fatty degeneration,* and the more generic *fatty infiltration* are consistently and interchangeably found in the literature. Muscle atrophy is a normal response to disuse, whether that disuse is caused by tenotomy-induced mechanical unloading[10] or inactivity[11], and under most conditions can be nearly reversed by muscle reloading[12]. In contrast, degeneration is an accumulation of muscle damage and cell death driven by multiple factors including inflammation, abnormal mechanical forces, and altered vascularization and is classically seen in the inflammatory myopathies and dystrophies[8,9]. It is indisputable that fat accumulates in diseased rotator cuff muscle. Indeed, clinical and surgical decisions are often made on the basis of computed tomography (CT) or magnetic resonance imaging (MRI) evaluation of the rotator cuff muscles, with Goutallier scores being the primary clinical measure of the rotator cuff muscle quality and overall disease severity[13,14].

Regarding the terms *fatty atrophy* versus *fatty degeneration,* previous studies of the relationship between muscle loss and fat accumulation are limited and have focused primarily on early to mid-stage rotator cuff disease. Those studies demonstrated decreased muscle fiber diameter[15] and specific force production[16] along with disrupted subcellular architecture, including small (~1-μm) lipid droplet accumulation in individual muscle fibers following a tendon tear[16,17]. No degenerative features such as myophagocytosis, disrupted muscle fiber membranes, split fibers, centralized nuclei, or other classic features of muscle degeneration-regeneration[6] have been reported[15-17]. While previous studies clearly demonstrated atrophic changes in the muscle, no clear evidence has emerged to suggest a degenerative mechanism of muscle loss.

To address these fundamental gaps in the literature regarding advanced rotator cuff disease, the aim of the current study was to histologically characterize the tissues found in the muscular spaces of patients with chronic and severe rotator cuff disease in order to determine whether degenerative processes are present in rotator cuff muscle. These data may provide evidence to challenge clinical assumptions about the state of muscle in rotator cuff disease and broaden our understanding of the relationships between muscle and fat in advanced rotator cuff disease.

Materials and Methods

Twenty-three patients undergoing reverse total shoulder arthroplasty (Table I) provided consent for muscle biopsy to be performed. Approval from the appropriate institutional review boards was obtained. A fellowship-trained shoulder surgeon assigned Goutallier scores[13] for each muscle on the basis of clinically indicated T1-weighted MRI or CT arthrogram images in the coronal and sagittal-oblique planes.

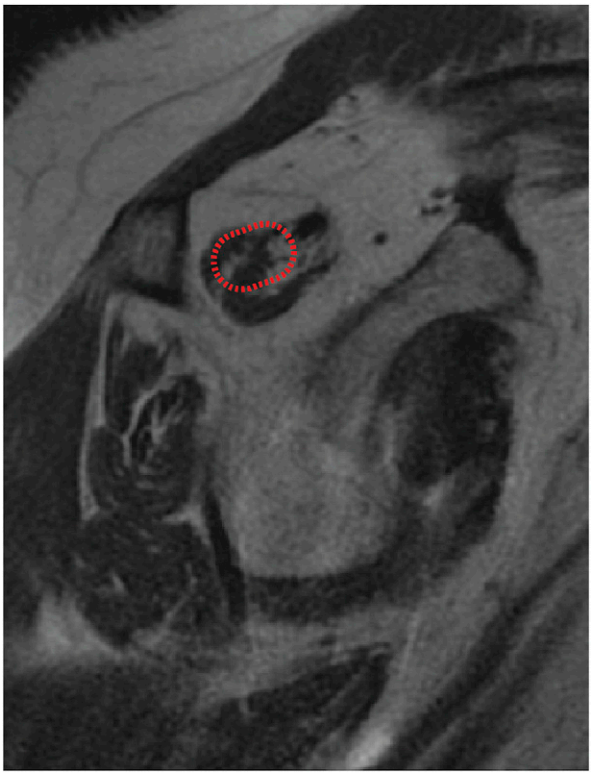

Fig. 1

Representative T1-weighted MRI showing the supraspinatus muscle biopsy region (red outline). The supraspinatus in this image had a Goutallier score of 3, and the biopsy sample did not contain identifiable muscle tissue.

TABLE II Histological Methods*

Dye or 1° Ab	2° Ab	Staining Protocol	Quantification
H & E	N/A	4 min hematoxylin 1 min LiCl soln. 3 sec eosin Dehydration Citrate clarifier Mount	Fascicles identified and scored as 1 or 0 for degeneration; intrafascicular and perifascicular fat quantified at ×10 and ×20 in Leica Digital Image Hub†
Gomori trichrome (in distilled H_2O: 6 g/mL chromatrope 2R, 3 g/mL aniline blue, 0.1 mL/mL glacial acetic acid, 8 g/mL phosphotungstic acid)	N/A	1 hr fixation in Bouin soln. H_2O wash 17.5 min trichrome 10 min Weigert hematoxylin Dehydration Mount†	ROI trace around sample area, manual thresholding of RGB channels (muscle = blue, loose connective tissue = green, and dense connective tissue = red) used to calculate area fractions of each tissue type within ROI. Each pixel counted for each tissue type independently†
CD68 (1:200) (Leica Biosystems/Novocastra CD68-L-CE)	Goat anti-mouse Alexa Fluor 488 (Invitrogen A11029) (1:400)	30 min 1% BSA-PBS Overnight 1° incubation in 0.1% BSA-PBS Wash 45 min 2° incubation Wash Mount	Particles in green channel with size range 10-200 μm^2 automatically identified, with manual removal of noncell particles preceding auto-quantification of macrophage density†§
α-SMA (1:200) (Diagnostic BioSystems MoB 001)	Goat anti-mouse Alexa Fluor 488 (Invitrogen A11029) (1:400)	30 min 1% BSA-PBS 1 hr 1° incubation in 0.1% BSA-PBS Wash 45 min 2° incubation Wash Mount	Particles in green channel with area >20 μm^2 automatically identified, with manual removal of nonvessel structures preceding auto-quantification of average vessel area and number†§
Perilipin (1:400) (Abcam ab3526)	Goat anti-rabbit Alexa Fluor 488 (Invitrogen A11008) (1:400)	Same as CD68	Used to confirm identity of lipid deposits in H & E and trichrome, and to evaluate the orientation of lipid relative to laminin muscle fiber borders†§
Laminin-211 (1:100) (Vector Laboratories VP-M648)	Goat anti-mouse Alexa Fluor 594 (Invitrogen A11032) (1:400)	Counterstain	Used to identify muscle fiber border to calculate muscle fiber area and centralized nuclei, counterstain for orientation in above stains†§
Laminin-111 (1:500) (Sigma L9393)	Goat anti-rabbit Alexa Fluor 594 (Invitrogen A11037) (1:400)	Counterstain	Used to identify muscle fiber border to calculate muscle fiber area and centralized nuclei, counterstain for orientation in above stains†§

*All quantification and manual screening performed by a single observer with 4 years of experience in muscle histology, blinded to Goutallier score and the intraoperative appearance of the muscle. 1° = primary; Ab = antibody; 2° = secondary; N/A = not applicable; LiCl = lithium chloride; ROI = region of interest; RGB = red, green, and blue; and BSA-PBS = bovine serum albumin-phosphate buffered saline solution. †H & E and trichrome stains were mounted with Permount mounting medium (Fisher Scientific) and imaged on a Leica SCN400 slide scanner. ‡Immunofluorescent stains were mounted with Vectamount mounting media with DAPI (Vector Laboratories) to visualize nuclei. All immunofluorescent imaging carried out on a Leica DM6000B microscope with DCF365FX camera on ×10 setting (×100 total magnification). §Tile imaging of entire cross-section and manual background adjustment were performed before quantification of all immunofluorescent images in ImageJ.

Using an anterosuperior approach, biopsy samples (ranging from 30 to 500 mg; mean diameter [and standard deviation] of 5.3 ± 2.0 mm) were collected under direct visualization from the scapular fossae, in a region defined by the lateral edge of the glenoid and no more than 2 cm medial from that landmark. Muscle that was macroscopically defined as pink-red organized fascicular tissue was specifically targeted; samples were not obtained

from muscles without such tissue. Obvious adipose or tendon tissue was avoided (Fig. 1). The supraspinatus was always evaluated and a biopsy sample obtained if it met the above-mentioned criteria, and in multiple cases, the infraspinatus (including the infraspinatus-teres minor junction) was evaluated and a sample obtained. Immediately after biopsy, samples were pinned under tension along the medial-lateral axis, flash-frozen in liquid nitrogen-cooled isopentane, transported on dry ice, and stored at −80°C.

Ten-micron sections embedded in OCT (optimum cutting temperature) compound were generated on a cryostat (CM3050 S; Leica). For each measurement, the entire area of a single cross-section (6 to 20 fields) was quantified by a single observer with 4 years of muscle histology experience who was blinded to the Goutallier score and the intraoperative appearance (Table II). All quantification was performed using automated procedures in ImageJ[18], which required only minimal input from the operator. Hematoxylin and eosin (H & E) and Gomori trichrome stains were used in evaluating the overall tissue composition and structure[19]. The relative fraction of organized, dense connective tissue; loose, disorganized tissue similar in appearance to granulation tissue; and muscle fibers was quantified on the basis of manual thresholding of staining color and intensity, where loose connective tissue was similar in color but lighter in shade and intensity than dense connective tissue because of the relative packing of the extracellular matrix (ECM). The same program was also used to quantify areas of fat within the sections.

To quantify the prevalence of degeneration and intrafascicular fat accumulation, each fascicle in an H & E-stained cross-section was scored for evidence of degenerating fibers and intrafascicular and perifascicular fat, with the results reported as a percentage of total fascicles per sample. In this analysis, muscle degeneration was defined as the presence of hypercellular infiltration of muscle fibers (i.e., myophagocytosis), the disrupted integrity of muscle fiber membranes, or split muscle fibers[6,9]. Intrafascicular fat was defined as large, eosin-negative cells residing within the perimysium, while perifascicular fat was defined as similarly eosin-negative cells in contact with, but not clearly within, the fascicular border. Immunostaining for the adipocyte lipid droplet protein perilipin (Abcam) was used to confirm that such eosin-negative cells contained lipid.

The number and size of noncapillary blood vessels (alpha-smooth muscle actin [α-SMA]; Diagnostic Biosystems) and the number of macrophages (CD68; Leica Biosystems/Novocastra) were quantified for whole biopsy cross-sections in ImageJ[20,21]. Samples were counterstained with laminin-111 or laminin-211 (LAMA1; Sigma, or LAMA2; Vector Laboratories) and 4',6-diamidino-2-phenylindole (DAPI).

The muscle fiber area and centralized nuclei were quantified via laminin and DAPI overlay using ImageJ[18]. The average muscle fiber area was weighted for total fiber area within each sample in order to account for varying amounts of muscle between samples. As a control group for muscle fiber area and central nuclei, 4 cadaveric supraspinatus muscles with no sign of rotator cuff disease were stained with H & E and quantified manually.

Statistical Analysis

Data are reported as the mean and standard deviation. Due to the differences in disease state between muscles, no pairwise correction was applied when multiple muscles from the same individual were biopsied. One or 2-way analyses of variance (ANOVAs) were used as appropriate to compare measurements between Goutallier scores, and Student t tests were used to compare patient biopsies with cadaveric data as well as muscle versus nonmuscle regions within the same biopsy samples. Linear regression was used to assess correlations between compositional parameters. Significance thresholds were set at an alpha level of 0.05.

Results

Of the total sample pool (n = 31), only 25.8% contained histologically identifiable muscle fibers. On average, the samples consisted of 48.2% ± 19.1% dense connective tissue, 36.9% ± 15.9% disorganized and loose connective tissue similar to granulation tissue, and only 10.4% ± 22.0% muscle overall (Fig. 2). Of the samples with any identifiable muscle tissue, the composition was 30.3% ± 11.8% dense connective tissue, 26.7% ± 17.4% loose connective tissue, and 40.1% ± 26.5% muscle. There was a significant interaction between biopsy sample composition and Goutallier score (p = 0.0027), with samples from muscles with lower Goutallier scores containing more muscle tissue on average, and with muscle tissue nearly absent in samples from muscles with a Goutallier score of 4. The average fat composition in all samples was low (6.5% ± 11.6%), which was likely due to our purposeful avoidance of macroscopic fat at biopsy sample collection.

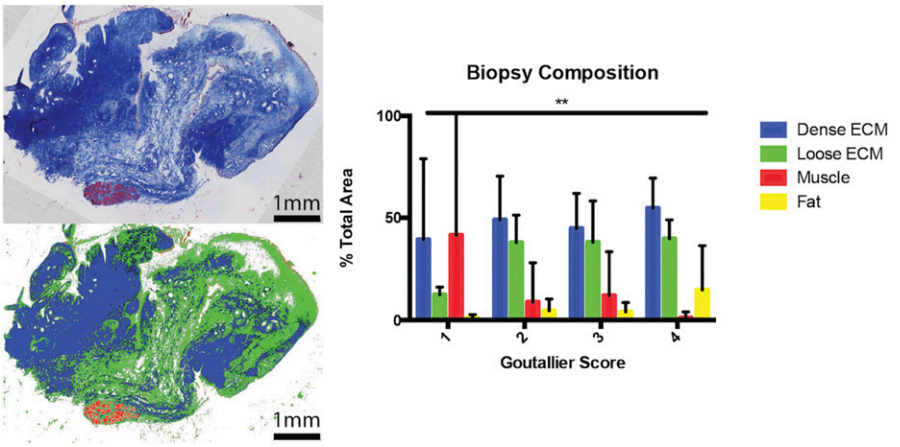

Fig. 2

Gomori trichrome-stained biopsy section demonstrating regions of dense connective tissue, loose connective tissue similar to granulation tissue, and muscle (**upper-left panel**); tissue fractions as classified by ImageJ, with muscle in red, organized connective tissue in blue, and loose connective tissue in green (**lower-left panel**); and biopsy composition grouped by Goutallier score, which demonstrated a significant interaction in 2-way ANOVA analysis (**p = 0.0027) (**right panel**). The error bars indicate the standard deviation.

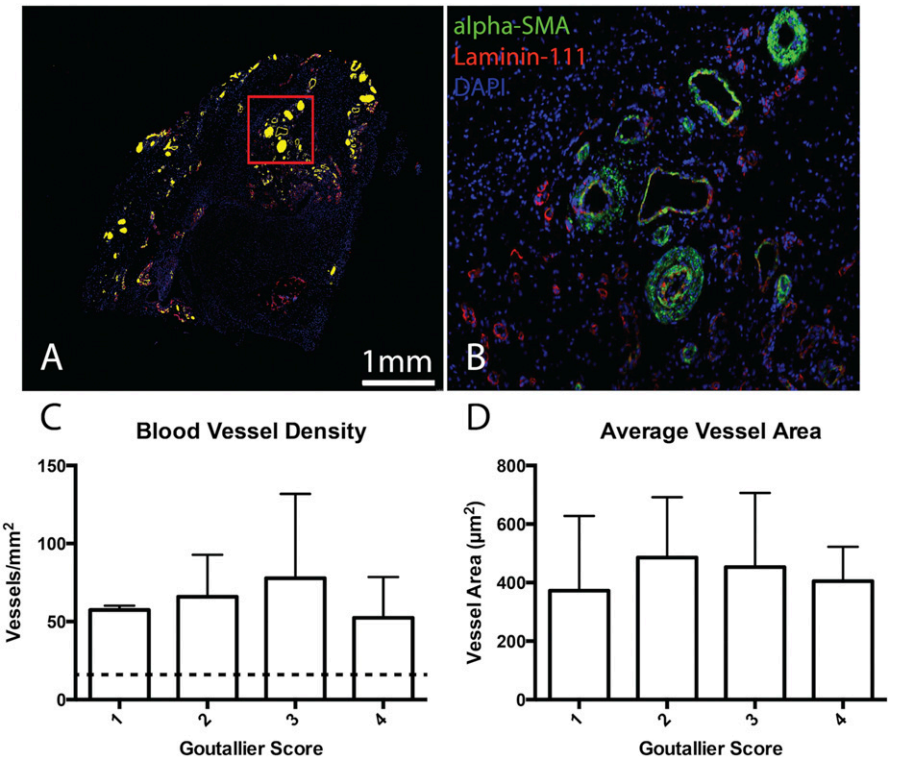

Fig. 3

A representative image showing alpha-smooth muscle actin (SMA) stain, with positive vessels shaded in yellow (**Fig. 3-A**); a ×100-magnified image of the region outlined in red in Figure 3-A, showing the alpha-SMA-positive vessels in green (**Fig. 3-B**); the average blood vessel density by Goutallier score, where the dashed line represents the vessel density reported for healthy muscle (**Fig. 3-C**); and the average vessel area by Goutallier score (**Fig. 3-D**). The error bars indicate the standard deviation.

Altered vascularization was prominent in the majority of samples, with an average vessel density among all samples of 66.6 ± 38.0 vessels/mm^2 and an average area per vessel of 448.7 ± 204.3 μm^2 (Fig. 3). This represents a 4-fold[20] to 130-fold[22] increase in the normal vessel density of skeletal muscle (dashed line in Figure 3-C, as measured in adult rat hindlimb muscle). No significant difference in vessel density was observed between samples with or without identifiable muscle tissue or on the basis of Goutallier scores.

Profound inflammation was observed (Fig. 4), with an average of 111.3 ± 81.5 macrophages/mm^2 across all samples and 103.3 ± 88.8 macrophages/mm^2 among the muscle-containing samples. This is 10-fold to 100-fold higher macrophage density than has been reported for either healthy

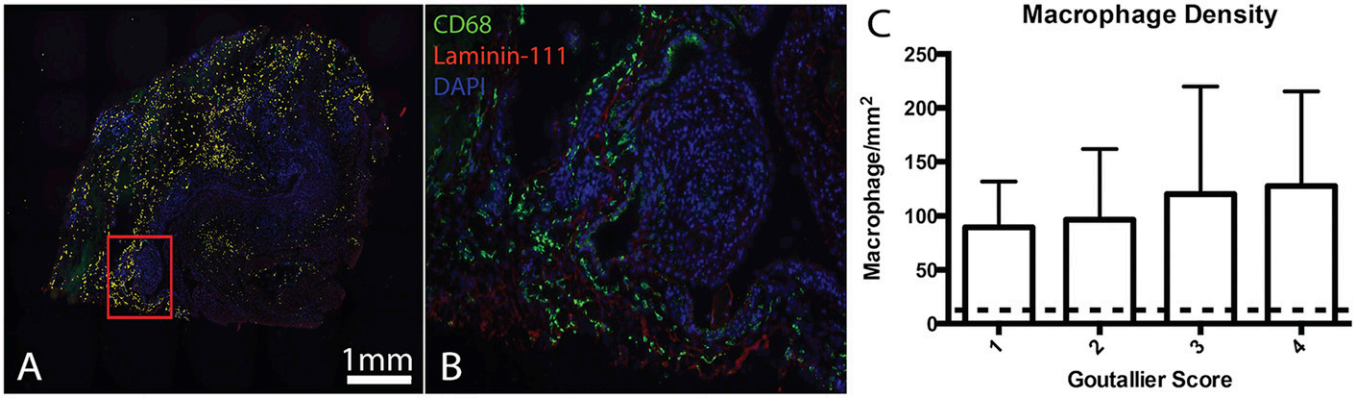

Fig. 4

A representative image showing CD68 stain with positive macrophages shaded in yellow (**Fig. 4-A**); a ×100-magnified image of the region outlined in red in Figure 4-A, showing CD68-positive macrophages in green (**Fig. 4-B**); and macrophage density by Goutallier score, where the dashed line represents the normal threshold for macrophages in muscle tissue (**Fig. 4-C**). The error bars indicate the standard deviation.

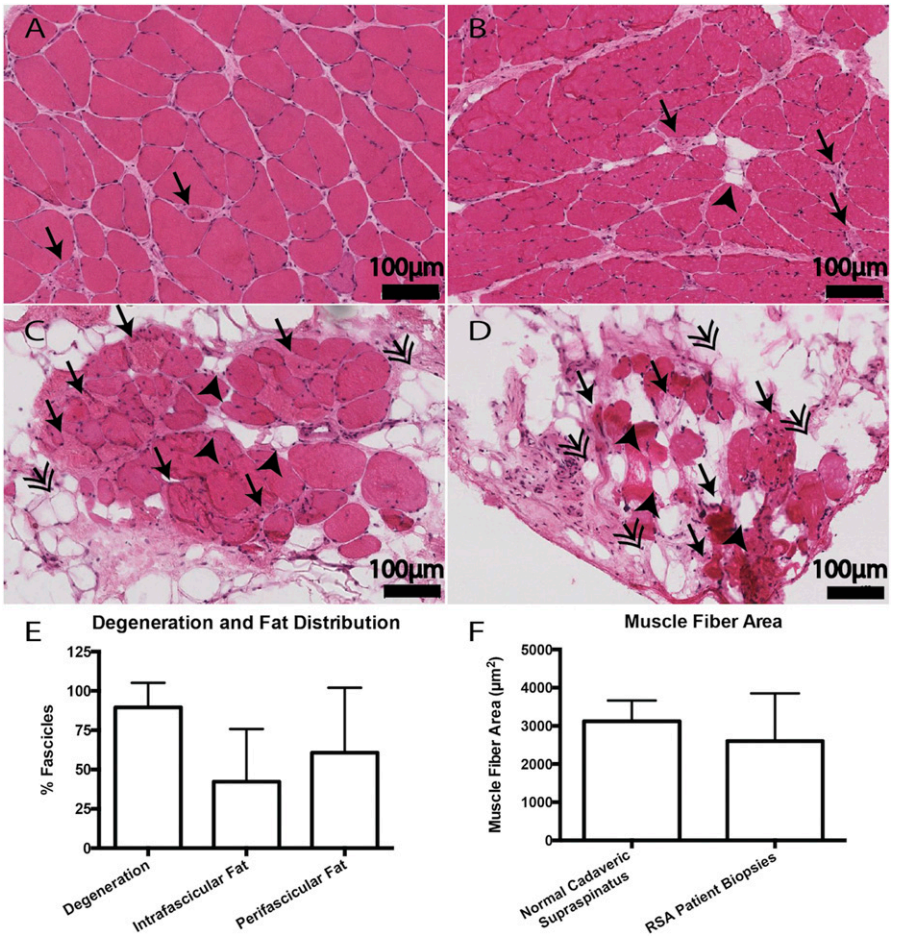

Fig. 5

Figs. 5-A through 5-D The range of degenerative changes observed (H&E staining). **Fig. 5-A** Limited degenerative signs (black arrows) and elevated central nuclei. **Fig. 5-B** Increasing degenerative signs with limited fat accumulation within the fascicle (black arrowheads). **Fig. 5-C** High levels of muscle degeneration and cellular invasion of muscle fibers (myophagocytosis), with greatly increased ECM and fat content both intrafascicularly (arrowheads) and perifascicularly (double arrowheads). **Fig. 5-D** Nearly complete loss of muscle with replacement by fat and fibrous tissue. **Fig. 5-E** Quantification of the percentage of total fascicles demonstrating muscle degeneration, intrafascicular fat, and perifascicular fat per sample. **Fig. 5-F** The average muscle fiber area weighted by total muscle area, compared with cadaveric controls. RSA = reverse shoulder arthroplasty. The error bars indicate the standard deviation.

muscle[23] or tendon[24] (1 to 10 macrophages/mm^2, dashed line in Figure 4-C). No significant difference was found in macrophage density across Goutallier scores or between samples with or without histological evidence of muscle. Furthermore, macrophage density was not significantly different in biopsy regions composed primarily of muscle compared

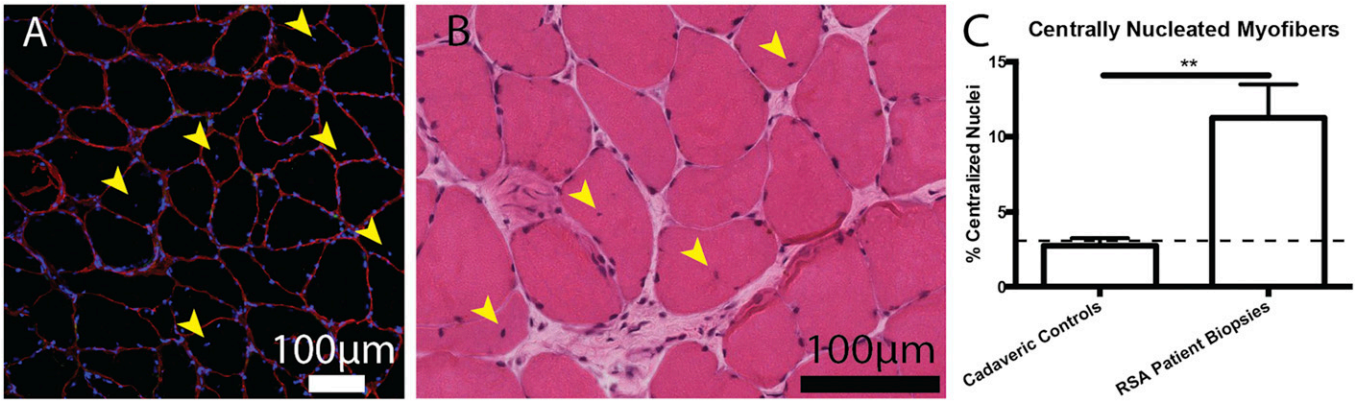

Fig. 6

Laminin-DAPI overlay image used to quantify central nuclei (yellow arrowheads) (**Fig 6-A**); ×20 magnification H & E-stained image of muscle fibers demonstrating centralized nuclei (yellow arrowheads) (**Fig. 6-B**); and the percentage of centrally nucleated muscle fibers within a sample, demonstrating significant pathological elevation compared with both cadaveric controls (**p = 0.0063) and the clinical standard for pathology (3%, dashed line) (**Fig. 6-C**). RSA = reverse shoulder arthroplasty. The error bars indicate the standard deviation.

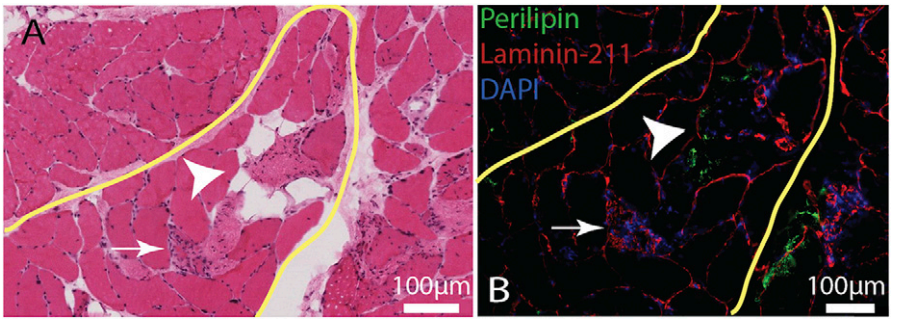

Fig. 7

Serial sections stained with H & E (**Fig. 7-A**) and perilipin counterstained with laminin and DAPI (**Fig. 7-B**) demonstrating a single muscle fascicle (yellow border) with a central region (white arrowhead) in which adipose tissue has directly replaced degenerating muscle (white arrow) without altering the structure of the fascicle (as quantified in Figure 5-E).

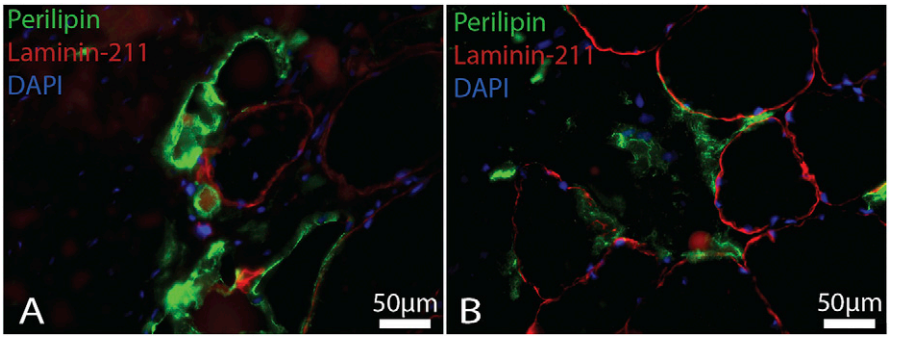

Fig. 8

Uniform perilipin-positive regions (green) demonstrating lipid accumulation in a geometry and location similar to that of surrounding muscle fibers (**Fig. 8-A**); and disrupted laminin border of muscle demonstrating positive perilipin staining suggestive of direct replacement of degenerating muscle by fat (**Fig. 8-B**).

with the cumulative macrophage density of the total sample cross-section.

Within regions containing identifiable muscle fibers, signs of muscle degeneration were observed in 90.0% ± 15.6% of all muscle fascicles (Fig. 5). These features qualitatively occurred more frequently around muscle-nonmuscle interfaces and within regions of high cellularity, although precise quantification of this phenomenon proved difficult. The percentage of centrally nucleated muscle fibers was also significantly elevated (11.3% ± 6.3%; $p = 0.0063$) compared both with the cadaveric controls (2.74% ± 1.0%) and the clinical threshold for abnormal central nuclei (3%)[25] (Fig. 6). Interestingly, no difference was found between biopsy samples and cadaveric controls in terms of the average muscle fiber area (Fig. 5-F), although this measurement was mildly underpowered ($\beta = 0.62$).

On average, adipose tissue was dispersed throughout the biopsy samples and constituted only a small fraction (6.5% ± 11.6%) of the total area sampled. In samples containing muscle fibers, although the total fat content remained low, fat was consistently concentrated at fascicular borders and between fascicles (perifascicular fat, 60.7% ± 41.4% of fascicles) as well as within fascicles (intrafascicular fat, 42.2% ± 33.6% of fascicles). Interestingly, intrafascicular fat was often seen in combination with degenerative signs, yet the endomysial and perimysial structures appeared intact (Figs. 7 and 8-A). In some cases, perilipin staining appeared to penetrate discontinuous laminin borders of muscle fibers (Fig. 8-B), although this phenomenon of fat infiltration of individual muscle fibers was rare and therefore difficult to quantify.

Discussion

In the presence of chronic and severe rotator cuff disease, the nonfatty tissues of the normally muscular supraspinatus and infraspinatus fossae were composed primarily of vascularized connective tissue. A large fraction of this tissue was similar in appearance to granulation tissue that forms in response to severe tissue damage, in that it was composed of vascular, loose connective tissue that has a high macrophage density[26]. This finding is not unprecedented given that chronic inflammation and muscle degeneration cause neovascularization while diminishing muscle volume[27,28]. Although tissue composition was related to Goutallier score, the assumptions about tissue type and quality that are associated with each scoring level are called into question. Because our biopsy procedure targeted only nonfatty tissue, low fat content relative to clinical images was expected. However, lack of muscle relative to what was

observed on imaging and intraoperatively may relate to the hypervascularity of the disorganized connective tissue. Additional research (high-resolution, quantitative MRI and histology) on isolated biopsy samples is needed to test this idea. Combined with the large number of actively degenerating muscle fibers observed, these data suggest that imaging may create considerable overestimation of the fraction of viable contractile tissue within the fossa.

While understanding tissue composition is critical to interpreting clinical images and making surgical decisions, elucidating the source of muscle loss is potentially a more important issue. Specifically, the distinction between the terms *fatty degeneration, fatty atrophy,* and *fatty infiltration* is rarely addressed in the literature. Although previously underappreciated, the implications of atrophy versus degeneration and fatty infiltration versus replacement are, in fact, critical in understanding disease progression on a cellular level.

The most appropriate term to describe the findings of previous studies in this area appears to be *fatty atrophy.* In evaluating the muscle of early-stage rotator cuff disease, Lundgreen et al. reported decreased muscle fiber diameter and increased perifascicular fat but found no evidence of degeneration-regeneration cycling as evidenced by a normal percentage of centrally nucleated muscle fibers[15]. Steinbacher et al. reported a similar increase in overall fat and perifascicular ECM, with increased lipid content and decreased myofibrillar organization in affected muscle fibers[17]. Mendias et al. corroborated these findings, and further showed diminished force production in muscle fibers isolated from chronic, full-thickness tears[16]. Animal models of rotator cuff disease, particularly large animal models, are relatively effective in recapitulating this atrophic, fat-accumulating phenotype of early and mid-stage disease[29-35]. However, to our knowledge, no previous study involving humans or animals has addressed the existence of degeneration or the tissue-level pattern of fat accumulation within the muscle in the most chronic and advanced stage of rotator cuff disease.

The data presented here provide clear evidence that muscle degeneration and regeneration occur in advanced rotator cuff disease. The level of muscle degeneration was profound, where 90% of fascicles displayed some degenerative features and 74% of the biopsy samples contained no muscle tissue at all, despite intraoperative targeting of muscle tissue. A previous study noted significant reductions in muscle fiber area between control samples and large tears[17], and although our mean muscle fiber areas were also lower on average, they were not significantly different from cadaveric controls. Because our study was underpowered, we do not claim that atrophy was absent in these biopsy samples.

Cumulatively these data suggest that imbalanced degeneration-regeneration, possibly exacerbated by high levels of inflammation, is the primary driver of muscle loss in later-stage rotator cuff disease. We speculate that this degenerative mechanism of muscle loss is somewhat similar to that of the inflammatory myopathies, and contrasts with the atrophy-driven muscle loss reported in early-stage disease[15]. Functionally, muscle loss from atrophy and degeneration will both result in impaired force production. The distinction between atrophy and degeneration has critical implications for recovery. An atrophic muscle may be rescued with renewed activation and mechanical reloading (i.e., tendon repair and exercise) even in older patients[12]. Conversely, a chronically degenerated muscle with cell loss and likely impaired regenerative capacity may be further damaged by the same treatment[36], with limited capacity to increase muscle fiber number. In the latter case, treatment with anti-inflammatory and/or pro-myogenic (pharmacological or cellular) therapies may be appropriate.

Of interest was the presence of fat in structures that appeared to be previously filled with contractile tissue, indicative of a more chronic and possibly terminal stage of degeneration. In addition to the *fatty infiltration* described ubiquitously in the literature, we demonstrated the proximity of degenerative fibers and large, lipid-filled structures within architecturally preserved fascicles in >40% of all fascicles. The origin of this lipid remains to be determined, but may be related to the lipid-laden macrophages described by Mendias et al.[16], as it is possible that such macrophages could differentiate into adipocytes[37]. More detailed analysis demonstrated perilipin-positive membranes surrounded by or crossing laminin borders, suggesting that the lipid deposit had replaced the contractile apparatus while maintaining the original muscle fiber structure. To our knowledge, this is the first human example of a muscle-to-fat transition that preserved the underlying muscle matrix architecture in what could be considered "fatty replacement." This phenomenon is not entirely unprecedented, as previous studies have shown adipogenic transition of both human myeloid cells[37] and resident muscle stem cells in rodent systems[38,39]. Additional studies that specifically trace cell fate are required to identify the exact cell source or sources of the accumulating fat, as it is possible that the fat in different anatomical locations or in distinct stages of disease is derived from divergent cell depots.

As with many studies of this nature, obtaining the appropriate control data proved difficult. Rotator cuff muscle-specific control data are absent in the literature, and due to limitations inherent to fixed tissue—specifically that extracellular and nonmuscle tissues (especially loose connective and adipose tissue) are severely disrupted and often destroyed in processing—and that immunohistochemical assays are largely ineffective on fixed tissue, we could not obtain meaningful control data for many of our assays.

Another limitation of this study was the relatively low number of biopsy samples that actually contained identifiable muscle fibers, particularly in the supraspinatus. This low muscle fraction was startling, given the MRI and intraoperative appearance of muscle-like tissue in the biopsy region. Although we can associate a biopsy region with an imaging-based region, we did not perform stereotactic biopsy (exact position). Nevertheless, the severe muscle degeneration measured here suggests that tissue quality is not well represented by current clinical imaging modalities. This in turn may help to explain the high number of unsatisfactory clinical outcomes. If the extent of muscle degeneration and replacement by

noncontractile tissue is systematically underestimated, which our data emphatically suggest, then standard treatments may insufficiently address the underlying pathology and functional deficits may persist even in the presence of an anatomically repaired cuff.

In summary, we demonstrated that rotator cuff muscle exhibits an active cycle of degeneration and regeneration in advanced rotator cuff disease, with degeneration potentially exacerbated by high levels of inflammation. Muscle loss in these samples was so profound that, in a large majority of the samples, muscle tissue was completely replaced by a disorganized, vascular connective-tissue network with high macrophage density. It is possible that such tissue appears similar to muscle in clinical imaging, leading to gross underestimation of muscle degeneration. We also provided evidence for the existence of a process of "fatty replacement," whereby degenerating muscle is replaced by fat while maintaining the structure of the native muscle fiber ECM. Clinically, these results indicate that more careful staging of muscle quality may be important for surgical decision-making, as the most severe forms of degeneration may not respond well to muscle reloading. ■

Michael C. Gibbons, MS[1]
Anshu Singh, MD[2]
Oke Anakwenze, MD[2]
Timothy Cheng, MD[1]
Maxwill Pomerantz, BS[1]
Simon Schenk, PhD[1]
Adam J. Engler, PhD[1]
Samuel R. Ward, PT, PhD[1]

[1]Departments of Bioengineering (M.C.G. and A.J.E.), Orthopaedic Surgery (T.C., M.P., S.S., and S.R.W.), and Radiology (S.R.W.), University of California San Diego, San Diego, California

[2]Kaiser Permanente, San Diego, California

E-mail address for S.R. Ward: srward@ucsd.edu

References

1. Yamamoto A, Takagishi K, Osawa T, Yanagawa T, Nakajima D, Shitara H, Kobayashi T. Prevalence and risk factors of a rotator cuff tear in the general population. J Shoulder Elbow Surg. 2010 Jan;19(1):116-20.

2. Bishop J, Klepps S, Lo IK, Bird J, Gladstone JN, Flatow EL. Cuff integrity after arthroscopic versus open rotator cuff repair: a prospective study. J Shoulder Elbow Surg. 2006 May-Jun;15(3):290-9.

3. Longo UG, Franceschi F, Ruzzini L, Rabitti C, Morini S, Maffulli N, Denaro V. Histopathology of the supraspinatus tendon in rotator cuff tears. Am J Sports Med. 2008 Mar;36(3):533-8. Epub 2007 Nov 15.

4. Riley GP, Goddard MJ, Hazleman BL. Histopathological assessment and pathological significance of matrix degeneration in supraspinatus tendons. Rheumatology (Oxford). 2001 Feb;40(2):229-30.

5. DE Giorgi S, Saracino M, Castagna A. Degenerative disease in rotator cuff tears: what are the biochemical and histological changes? Joints. 2014 Jan-Mar;2(1):26-8. Epub 2014 May 8.

6. Dubowitz V, Sewry CA, Oldfors A. Muscle biopsy: a practical approach. 4th ed. Philadelphia: Elsevier Health Sciences; 2013.

7. Bonaldo P, Sandri M. Cellular and molecular mechanisms of muscle atrophy. Dis Model Mech. 2013 Jan;6(1):25-39.

8. Wallace GQ, McNally EM. Mechanisms of muscle degeneration, regeneration, and repair in the muscular dystrophies. Annu Rev Physiol. 2009;71:37-57.

9. Preedy VR, Peters TJ. Skeletal muscle: pathology, diagnosis and management of disease. New York: Cambridge University Press; 2002.

10. Thomason DB, Booth FW. Atrophy of the soleus muscle by hindlimb unweighting. J Appl Physiol (1985). 1990 Jan;68(1):1-12.

11. Levine S, Nguyen T, Taylor N, Friscia ME, Budak MT, Rothenberg P, Zhu J, Sachdeva R, Sonnad S, Kaiser LR, Rubinstein NA, Powers SK, Shrager JB. Rapid disuse atrophy of diaphragm fibers in mechanically ventilated humans. N Engl J Med. 2008 Mar 27;358(13):1327-35.

12. Frontera WR, Meredith CN, O'Reilly KP, Knuttgen HG, Evans WJ. Strength conditioning in older men: skeletal muscle hypertrophy and improved function. J Appl Physiol (1985). 1988 Mar;64(3):1038-44.

13. Goutallier D, Postel JM, Bernageau J, Lavau L, Voisin MC. Fatty muscle degeneration in cuff ruptures. Pre- and postoperative evaluation by CT scan. Clin Orthop Relat Res. 1994 Jul;304:78-83.

14. Fuchs B, Weishaupt D, Zanetti M, Hodler J, Gerber C. Fatty degeneration of the muscles of the rotator cuff: assessment by computed tomography versus magnetic resonance imaging. J Shoulder Elbow Surg. 1999 Nov-Dec;8(6):599-605.

15. Lundgreen K, Lian ØB, Engebretsen L, Scott A. Lower muscle regenerative potential in full-thickness supraspinatus tears compared to partial-thickness tears. Acta Orthop. 2013 Dec;84(6):565-70. Epub 2013 Oct 31.

16. Mendias CL, Roche SM, Harning JA, Davis ME, Lynch EB, Sibilsky Enselman ER, Jacobson JA, Claflin DR, Calve S, Bedi A. Reduced muscle fiber force production and disrupted myofibril architecture in patients with chronic rotator cuff tears. J Shoulder Elbow Surg. 2015 Jan;24(1):111-9. Epub 2014 Sep 3.

17. Steinbacher P, Tauber M, Kogler S, Stoiber W, Resch H, Sänger AM. Effects of rotator cuff ruptures on the cellular and intracellular composition of the human supraspinatus muscle. Tissue Cell. 2010 Feb;42(1):37-41. Epub 2009 Aug 25.

18. Abramoff MD, Magalhães PJ, Ram SJ. Image processing with ImageJ. Biophotonics International. 2004 Jul;11(7):36-42.

19. Miller JL, Watkin KL, Chen MF. Muscle, adipose, and connective tissue variations in intrinsic musculature of the adult human tongue. J Speech Lang Hear Res. 2002 Feb;45(1):51-65.

20. Hansen-Smith F, Egginton S, Hudlicka O. Growth of arterioles in chronically stimulated adult rat skeletal muscle. Microcirculation. 1998;5(1):49-59.

21. Pulford KA, Sipos A, Cordell JL, Stross WP, Mason DY. Distribution of the CD68 macrophage/myeloid associated antigen. Int Immunol. 1990;2(10):973-80.

22. Laughlin MH, Cook JD, Tremble R, Ingram D, Colleran PN, Turk JR. Exercise training produces nonuniform increases in arteriolar density of rat soleus and gastrocnemius muscle. Microcirculation. 2006 Apr-May;13(3):175-86.

23. Dorph C, Englund P, Nennesmo I, Lundberg IE. Signs of inflammation in both symptomatic and asymptomatic muscles from patients with polymyositis and dermatomyositis. Ann Rheum Dis. 2006 Dec;65(12):1565-71. Epub 2006 Jul 10.

24. Matthews TJ, Hand GC, Rees JL, Athanasou NA, Carr AJ. Pathology of the torn rotator cuff tendon. Reduction in potential for repair as tear size increases. J Bone Joint Surg Br. 2006 Apr;88(4):489-95.

25. Sorarù G, D'Ascenzo C, Polo A, Palmieri A, Baggio L, Vergani L, Gellera C, Moretto G, Pegoraro E, Angelini C. Spinal and bulbar muscular atrophy: skeletal muscle pathology in male patients and heterozygous females. J Neurol Sci. 2008 Jan 15;264(1-2):100-5. Epub 2007 Sep 12.

26. Clark R. The molecular and cellular biology of wound repair. New York: Springer; 2013.

27. Jackson JR, Seed MP, Kircher CH, Willoughby DA, Winkler JD. The codependence of angiogenesis and chronic inflammation. FASEB J. 1997 May;11(6):457-65.

28. Conn PM. Methods in neurosciences. Vol 8, Neurotoxins. Atlanta: Elsevier Science; 1992.

29. Liu X, Manzano G, Kim HT, Feeley BT. A rat model of massive rotator cuff tears. J Orthop Res. 2011 Apr;29(4):588-95. Epub 2010 Oct 14.

30. Gerber C, Meyer DC, Schneeberger AG, Hoppeler H, von Rechenberg B. Effect of tendon release and delayed repair on the structure of the muscles of the rotator cuff: an experimental study in sheep. J Bone Joint Surg Am. 2004 Sep;86(9):1973-82.

31. Gumucio JP, Davis ME, Bradley JR, Stafford PL, Schiffman CJ, Lynch EB, Claflin DR, Bedi A, Mendias CL. Rotator cuff tear reduces muscle fiber specific force production and induces macrophage accumulation and autophagy. J Orthop Res. 2012 Dec;30(12):1963-70. Epub 2012 Jun 13.

32. Safran O, Derwin KA, Powell K, Iannotti JP. Changes in rotator cuff muscle volume, fat content, and passive mechanics after chronic detachment in a canine model. J Bone Joint Surg Am. 2005 Dec;87(12):2662-70.

33. Kim HM, Galatz LM, Lim C, Havlioglu N, Thomopoulos S. The effect of tear size and nerve injury on rotator cuff muscle fatty degeneration in a rodent animal model. J Shoulder Elbow Surg. 2012 Jul;21(7):847-58. Epub 2011 Aug 10.

34. Rowshan K, Hadley S, Pham K, Caiozzo V, Lee TQ, Gupta R. Development of fatty atrophy after neurologic and rotator cuff injuries in an animal model of rotator cuff pathology. J Bone Joint Surg Am. 2010 Oct 6;92(13):2270-8.

35. Gerber C, Schneeberger AG, Perren SM, Nyffeler RW. Experimental rotator cuff repair. A preliminary study. J Bone Joint Surg Am. 1999 Sep;81(9):1281-90.

36. Garrett WE, Kirkendall DT. Exercise and sport science. Philadelphia: Lippincott Williams & Wilkins; 2000.

37. Majka SM, Fox KE, Psilas JC, Helm KM, Childs CR, Acosta AS, Janssen RC, Friedman JE, Woessner BT, Shade TR, Varella-Garcia M, Klemm DJ. De novo generation of white adipocytes from the myeloid lineage via mesenchymal intermediates is age, adipose depot, and gender specific. Proc Natl Acad Sci U S A. 2010 Aug 17;107(33):14781-6. Epub 2010 Aug 2.

38. Asakura A, Komaki M, Rudnicki M. Muscle satellite cells are multipotential stem cells that exhibit myogenic, osteogenic, and adipogenic differentiation. Differentiation. 2001 Oct;68(4-5):245-53.

39. Uezumi A, Ikemoto-Uezumi M, Tsuchida K. Roles of nonmyogenic mesenchymal progenitors in pathogenesis and regeneration of skeletal muscle. Front Physiol. 2014;5:68.